

# When Memristance Crosses the Path with Humidity Sensing—About the Importance of Protons and Its Opportunities in Valence Change Memristors

Felix Messerschmitt, Maximilian Jansen, and Jennifer L. M. Rupp\*

Resistive switching devices based on oxides have outstanding properties, making them a promising candidate to replace today's transistor-based computer memories as non-volatile valence change memories, and can even find future application in neuromorphic computing. To date, the scientific discussion is so far mainly restricted to oxygen vacancy contributions disregarding the role of protonic defects on resistive switching. In this work, the effect of moisture and protonic contributions on resistive switching by changes in the surface to bulk ratio and oxide surface exposure of the oxide  $\text{SrTiO}_3$  is studied. Here, a linear to exponential SET current density dependency, when changing the film thickness by a factor of four, is found, whereby the surface-to-bulk ratio of the oxide is significantly changed. This behavior is discussed in terms of differences in total concentration of oxygen vacancies and their interplay with moisture. For classic memristor applications, this study demonstrates that protonic defects need to be accounted for memristor characteristics, as they crucially influence the switching characteristics, and give new opportunities as an additional handle to actively tune the switching performance. This memristive dependency on protonic defects opens a whole plethora of new modulatable sensor characteristics like creating humidity sensors using the property of memristance.

## 1. Introduction

Resistive switching devices are a promising alternative to replace today's transistor-based memory technology due to their superior properties such as low power consumption,

high switching speed, nonvolatility, and scalability.<sup>[1]</sup> These devices were linked to the exciting concept of memristors,<sup>[2–6]</sup> which not only exhibit superior memory properties but are also considered to be a crucial part in neuromorphic computing hardware because of their outstanding properties, such as spike time dependent plasticity or the capability of multilevel data storage.<sup>[7]</sup> These devices consist of a simple metal|oxide|metal structure, for which in valence change memories the metal electrodes are selected to be inactive, e.g., by the choice of platinum.<sup>[8]</sup> Here, under high electrical field, typically in the range of  $>10^6 \text{ V m}^{-1}$ ,<sup>[8,9]</sup> the defects become mobile within the metal oxide and are altering the overall resistance state of the memristor. Despite the exciting switching performances reported in literature there are still many obstacles to overcome such as endurance, variability, and uniformity issues.<sup>[10]</sup> Therefore it is essential to get a better understanding of the underlying fundamentals and to unveil the defect chemistry of metal oxide-based

thin films under high electrical fields at ambient conditions. In particular the role of defects, i.e., oxygen vacancies, protonic species, and electronic carriers within the metal oxide require attention as they define the final memristive characteristics. Fundamental studies on memristors predominantly address the interplay of oxygen vacancies and electronic carriers within the metal-oxide toward memristance.<sup>[11]</sup> However, contributions of protonic defects and their interplay with oxygen vacancies and electronic carriers are only rarely considered. Even though protonic defects are omnipresent in metal oxide thin films introduced either by the fabrication process and handling of the devices or through the reaction of atmospheric species like moisture during operation. Through this work we therefore focus on bipolar resistive switching valence change memories to study the role of protonic defects to memristance and its electric response for strontium titanate,  $\text{SrTiO}_3$ .

For this, we fabricate switching devices based on  $\text{SrTiO}_3$ , which is a well-suited model material and memristive oxide. The selected oxide is a mixed conductor with electronic p-type conduction at ambient conditions with a low cationic mobility when compared to the mobility of oxygen anions.<sup>[12]</sup> The cubic perovskite crystal structure of  $\text{SrTiO}_3$  is stable over a wide

Dr. F. Messerschmitt, M. Jansen, Prof. J. L. M. Rupp  
Electrochemical Materials  
Department of Materials  
ETH Zurich  
Hönggerbergstr. 64, 8093 Zurich, Switzerland  
E-mail: jrupp@mit.edu

Dr. F. Messerschmitt, Prof. J. L. M. Rupp  
Electrochemical Materials  
Department of Material Sciences and Engineering  
Massachusetts Institute of Technology  
77 Massachusetts Ave, Cambridge, MA 02139, USA

Dr. F. Messerschmitt, Prof. J. L. M. Rupp  
Electrochemical Materials  
Department of Electrical Engineering and Computer Science  
Massachusetts Institute of Technology  
77 Massachusetts Ave, Cambridge, MA 02139, USA

DOI: 10.1002/aelm.201800282

range of oxygen partial pressure and temperature.<sup>[13]</sup> Hence, resistance changes due to phase changes of the oxide or movement of the cations induced by the high electrical fields and local Joule heating can be ruled out. This is an important aspect since it allows simplifying the mechanistic discussion to the valence change mechanism. The defect chemistry of SrTiO<sub>3</sub> especially for high temperatures and low electrical fields is well established, e.g., we refer here for details to the excellent work of De Souza et al.<sup>[14]</sup> and Merkle and Maier.<sup>[15]</sup> Additionally, there exist many reports in literature pointing out the switching capabilities of SrTiO<sub>3</sub> with remarkable ratios of high and low resistance states,  $R_{\text{OFF}}/R_{\text{ON}}$ , of up to  $10^5$ ,<sup>[16]</sup> switching speeds of <100 ns,<sup>[17]</sup> retention >10 years,<sup>[18]</sup> and endurance of > $10^6$  cycles.<sup>[18]</sup> Moreover, the wealth of experience in working with SrTiO<sub>3</sub> as a transistor gate oxide on a chip<sup>[19]</sup> makes its integration into future memory devices highly feasible.

On closer inspection of literature it is obvious that the resistive switching mechanism of SrTiO<sub>3</sub>-based devices was already addressed in numerous experimental and theoretical studies in prior art, we refer here to Waser et al.<sup>[8]</sup> and Menzel et al.<sup>[17]</sup> A common view is that positively charged oxygen vacancies are accumulating in locally defined sites through the external electrical field applied forming conductive filaments lowering the overall resistance of the device. By applying the opposite polarity to the device these filaments get partially dissolved again resetting the device back to a high resistance state, which results in bipolar memristance. The importance of oxygen vacancy diffusion and oxygen vacancy-based filaments in SrTiO<sub>3</sub>-based memristors was shown in electrocoloration,<sup>[20]</sup> conductive atomic force microscopy,<sup>[21]</sup> chronoamperometry,<sup>[22]</sup> and in numerous cyclic voltammetry experiments.<sup>[16,18,22a,23]</sup> It should be mentioned that for SrTiO<sub>3</sub> devices these filaments do not give a complete picture of the oxygen vacancy defect chemistry involved in the reversible resistance changes. A second counteracting mechanism with a reverse bias polarity dependency and slower kinetics<sup>[24]</sup> than the filament formation can be triggered either by applying higher electrical fields than necessary for the formation of filaments<sup>[21a,24,25]</sup> or slower sweep rates<sup>[24]</sup> in cyclic voltammetry operation.

Despite these fundamental studies on the role of oxygen vacancies, there exist only a few reports examining the defect chemistry, kinetics, and additional types of defects such as *protonic defects* and their role contributing to memristive behavior of valence change memories. Even though it is well known that memristive oxides like SrTiO<sub>3</sub> vary its charge transport and electrical behavior with respect to atmospheric species like moisture<sup>[26]</sup> which also holds for many other memristive oxides such as CeO<sub>2</sub>,<sup>[27]</sup> TiO<sub>2</sub>,<sup>[28]</sup> BaTiO<sub>3</sub>,<sup>[29]</sup> and SnO<sub>2</sub>.<sup>[30]</sup> This dependency is for example even exploited in *resistive humidity sensors* where protonic defects are altering the overall conductivity and electrical properties of the oxide.<sup>[31]</sup> Most of such commercially available humidity sensors are based on the impedance change of the oxide upon moisture and are operated in the range of 10–95% relative humidity with typical response times of 20–30 s from ambient up to 400 °C.<sup>[32]</sup> For an excellent overview on the recent progress of ceramic based humidity sensors we refer to ref. [32]. In the sensor literature the defect chemistry including the reaction of SrTiO<sub>3</sub> to humidity changes and role of its protonic defects is well described for small external electrical fields, see refs. [15,33] for details. It was found that

the increased conductivity of oxides upon moisture exposure can originate from various conduction mechanisms.

First, chemisorbed water molecules on the surface of the oxide can facilitate the proton conduction via the “Grotthuss mechanism.”<sup>[33b,34]</sup> Depending on the water coverage at the surface additional physisorbed water can increase the conductivity.<sup>[35]</sup> The role of the oxides’ surfaces in the incorporation of protons and protonic conduction can also be seen in conductivity changes of metal oxides in dependence of their porosity and grain boundary density.<sup>[31a,36]</sup> Second, the water can be incorporated within the bulk through a hydration reaction increasing the protonic carrier concentration in the oxide. Here water from the gas phase dissociates through a surface oxygen vacancy assisted incorporation process into a hydroxide ion and a proton.<sup>[15,37]</sup> Experiments with minor doped iron SrTiO<sub>3</sub> single crystal samples revealed at low electrical fields nonmonotonous conductivity changes through the bulk caused by the three defect diffusion equilibrium of holes, protons, and oxygen vacancies.<sup>[33a,38]</sup> These changes in impedance upon moisture exposure in the metal oxide are then exploited in humidity sensors.

Unfortunately, the interaction of the surface with humidity is rarely investigated for memristors at high electrical fields and ambient conditions, even though it is known from catalysis that it can severely define i) the formation of oxygen defects at surface and bulk and ii) the incorporation of protonic defects into the lattice as third carrier species besides oxygen ions and electrons. Therefore we focus in this study on protonic carrier contribution to memristance and the interplay of moisture from the atmosphere with the memristive oxide. In general, such protonic defect contributions are omnipresent for oxide-based memristors, since it is difficult to fully avoid moisture due to its strong adhesion. For example, chemisorbed water on SrTiO<sub>3</sub> single crystalline samples was reported even for temperatures higher than 550 °C and at high vacuum atmosphere of  $2 \times 10^{-7}$  bar.<sup>[39]</sup> Moisture is typically present in the fabrication process of memristors, for example, during the photolithography in nanostructuring of the devices.<sup>[40]</sup> Additionally, prototype devices in fundamental studies are usually not encapsulated and therefore moisture from the atmosphere can freely interact with the samples during operation and handling at ambient conditions.

The importance of protonic defects in memristors was already highlighted for memristive materials such as TiO<sub>2</sub><sup>[41]</sup> and SiO<sub>2</sub>,<sup>[42]</sup> even though these are clearly not the dominant charge carriers. Jameson et al. who even considered protons as the responsible species for memristive behavior in TiO<sub>2</sub>.<sup>[41a]</sup> In a recent work we exemplified on the memristive oxide SrTiO<sub>3</sub> that moisture has a direct effect on the electrical properties and the memristive characteristics of valence change based memristors at operating conditions present during resistive switching, in particular at high local electrical fields and ambient for SrTiO<sub>3</sub>.<sup>[43]</sup> We reported that the memristive behavior vanished during cyclic voltammetry experiments in dry atmosphere (H<sub>2</sub>O < 3 ppm) and showed complicated multicrossing current–voltage profiles in humidified atmosphere. The maximum conductivity of the device reversibly shifted by significant four orders of magnitude for a change in relative humidity from 0% to 100% at room temperature. These results exemplified the

direct implication of the surface dissociation of water on SrTiO<sub>3</sub> on its property of memristance and also its interplay with oxygen vacancies and electronic carriers due to the charge balance. We concluded that not only oxygen vacancies but atmospheric species are interfering with the memristive performance and highlighted that memristance cannot solely be explained by oxygen vacancy kinetics for SrTiO<sub>3</sub>-based devices. This is now also supported by follow up studies on other valence change oxides, e.g., on TaO<sub>2</sub><sup>[44]</sup> and TiO<sub>2</sub><sup>[45]</sup> Despite the proof-of-concept that protonic carriers interfere with the memristive property of oxides following points remained unclear, which we want to address in this study on the example of SrTiO<sub>3</sub>-based memristors: i) Where and how do protons interfere with the memristance in memristors in detail? The possibility that the overall bulk charge carrier concentration of the oxide thin film is changed by the protonic lattice incorporation requires investigation. Alternative hypothesis is that the incorporation could be limited to the vicinity of the electrode|oxide interface. In this hypothesis the space charge region would be actively altered resulting in changes of the resistive switching profile with change in humidity. ii) What is the level of relative humidity at which the reported transition from memristive to solely capacitive behavior of the devices is observed? iii) How does the electrical field applied during the memristive operation at ambient conditions interfere with the moisture surface dissociation reaction? iv) Finally, can such parasitic atmosphere sensitivity be controlled for memory application by capping layers? Understanding the exact role of protonic defects interfering with oxygen vacancies at high electrical fields is of importance to assure a good and controllable memristive performance and stability. As an outcome of the work, we also will highlight the possibility to even extend the range of application of memristors, namely, as novel classes of memristive-operating sensing devices.

To this end, we turn to SrTiO<sub>3</sub> and *design a model experiment* on moisture influencing memristors to investigate two aspects in detail:

First, the *influence of surface to bulk ratio of the memristive oxide thin film on memristance in dependence of the moisture exposure is studied*. Therefore we fabricate two sets of memristor arrays, which exclusively differ in their thickness. By choosing thin film layer thicknesses one close to the Debye length,  $\approx 100$  nm,<sup>[46]</sup> with a *high surface to bulk ratio*, *HSBR*, and a second oxide film layer thickness far away of the Debye length<sup>[46]</sup> with a *low surface to bulk ratio*, *LSBR*. Through those model structures we are able to study the contributions of the Pt|SrTiO<sub>3</sub> interface and the bulk toward moisture. Here, we investigate the role of protonic defects toward memristive behavior by changing the relative humidity by small increments over a wide range of 0–80% during cycling voltammetry experiments on *HSBR* and *LSBR* samples. We analyze and discuss the memristive behavior of these memory arrays with respect to changes in current density, hysteretic *I*–*V* behavior, and sensitivity to moisture. Furthermore, we elucidate through these experiments the precise transition region at which the memristive behavior upon moisture exposure vanishes and solely capacitive behavior is observable.

Second, the *influence of an additional oxide capping layer on the property of memristance is investigated*. This allows studying how the electrical field interferes with the moisture incorporation and its kinetics into the memristive oxide, namely SrTiO<sub>3</sub>,

In addition we are evaluating if through such a simple encapsulation approach the memristive behavior can be controlled for memory application. Here, we fabricate a set of Pt|SrTiO<sub>3</sub>|Pt samples with equivalent oxide thickness and microstructure but with either *exposed memristive bits* which have a direct reaction path with atmospheric moisture or with *encapsulated memristive bits* by fabricating an additional not patterned SrTiO<sub>3</sub> capping layer on top. Through this approach we are able to demonstrate that the sensitivity upon moisture during memristive operation is highly tunable in oxide-based valence change memories and elucidate the importance of understanding protonic contributions toward the memristive mechanism.

Ultimately, we demonstrate as a proof-of-concept that Pt|SrTiO<sub>3</sub>|Pt structures have besides its exciting memristive characteristics the potential to be exploited either as *responsive moisture sensor units operating on memristance* (as a counterpart to classic resistivity or capacitance change) or even *combined memristive information processing and moisture sensing devices* for novel device functionalities and applications in the future. In addition, the results contribute to the understanding on how humidity interacts with a memristive material under bias such as by the nature of protonic species coupling at the oxide surface and toward its bulk.

## 2. Results and Discussion

### 2.1. Memristor Fabrication and Structural Characterization of the Devices

We successfully fabricated two-terminal Pt|SrTiO<sub>3</sub>|Pt memory arrays with either a high surface to bulk ratio, *HSBR*, or a low surface to bulk ratio, *LSBR*, which exclusively differ in their thickness. This approach allows gaining insights on *the bulk and surface contributions on moisture sensitivity of valence change-based memristors*. We also add to the *exposed HSBR* samples an *encapsulated HSBR* SrTiO<sub>3</sub>|Pt|SrTiO<sub>3</sub>|Pt reference sample. These structures allow studying *the influence of free surfaces on the property of memristance during the exchange with humid atmosphere under high electrical fields*. In addition we are evaluating if through such a simple encapsulation approach the memristive behavior can be controlled for memory application.

The *HSBR* samples reveal an oxide thickness of 170 nm close to the Debye length of SrTiO<sub>3</sub> ( $\approx 100$  nm),<sup>[47]</sup> whereas the *LSBR* samples have a four times increased oxide thickness of 740 nm (see schematic in **Figure 1a**). The encapsulation of the *HSBR* samples is achieved by depositing a capping layer on top (viz. a second SrTiO<sub>3</sub> oxide film of 150 nm) (**Figure 1a**). The oxide layers, including the capping layer, were not patterned and have a diameter of 2 cm, therefore a direct reaction path of the atmosphere with the bottom electrode can be ruled out for all our device structures. We engineer, for this model experiment various electrode configurations on the memory arrays to enable access to each single Pt top electrode of a “switching bit” in the configuration of Pt|SrTiO<sub>3</sub>|Pt. Here, we keep always the crossmeasurement geometry, measuring across the SrTiO<sub>3</sub> oxide layer accessing over a top Pt electrode and a bottom Pt electrode, denoted by the shorts “TE” and “BE” in **Figure 1b**. For this, the metal oxide films were fabricated via PLD with the

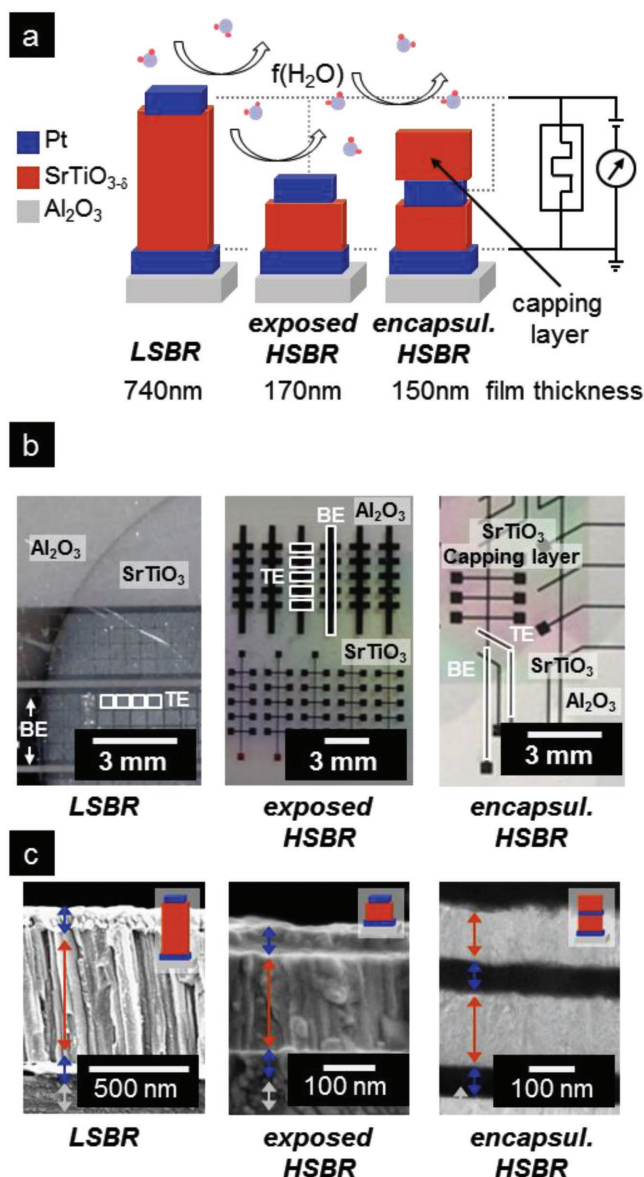


**Figure 1.** a) Schematic representation of SrTiO<sub>3</sub> thin film samples to vary the reaction pathways toward humidity during resistive switching experiments. For this, the prime model samples differ in i) surface to bulk ratio (LSBR/HSBR) and ii) with variation of the occurrence of the SrTiO<sub>3</sub> capping layer (exposed/encapsulated) for resistive switching measurements carried out with respect to moisture levels. b) Top view optical microscopy images of the three model samples showing the electrode designs with electrode areas of 500<sup>2</sup> and 25<sup>2</sup> μm<sup>2</sup>. c) Scanning electron microscope (SEM) crossview images of uncapped samples (left and middle) and transmission electron microscopy (TEM) image of an encapsulated sample (right) showing the polycrystalline columnar microstructure of oxide thin films and stack thereof. LSBR: low surface to bulk ratio (740 nm film thickness); HSBR: high surface to bulk ratio (170 nm film thickness); encapsul.: encapsulated sample.

same deposition parameters, only the number of laser shots was varied. This fabrication approach ensures that the sets of samples only differ in their surface to bulk ratio and atmosphere exposure level during the measurements, allowing us to limit the discussion of differences in their memristive behavior

to the interaction of humidity at the surface versus bulk interaction and the role of exposed and encapsulated surfaces.

Figure 1c shows the scanning electron microscopy and transmission electron microscopy images for the cross-sections of the samples verifying the targeted film thickness of the fabricated devices. The cross-section images confirm a dense equivalent polycrystalline columnar microstructure throughout the whole oxide film for all three sets of samples as expected from PLD growth on sapphire substrates. The images were taken after the electrical measurements showing no microstructural change in the oxide and intact electrodes. The cubic perovskite crystal structure of SrTiO<sub>3</sub> with a <111> preferential grain orientation perpendicular to the substrate was confirmed for all samples without any additional phases by X-ray diffraction measurements (see Figure S1, Supporting Information).

## 2.2. Moisture Sensitivity of Memristive Bits in Dependence of Surface to Bulk Ratio and Atmosphere Exposure

In the following, we investigate: i) the influence of a changed surface to bulk ratio on the property of memristance in dependence of the moisture exposure level and ii) the influence of an additional oxide capping layer on the characteristic of memristance. For this the relative humidity is systematically varied and the memristive behavior of the fabricated Pt|SrTiO<sub>3</sub>|Pt memory arrays is measured via cyclic voltammetry for seven distinct humidity levels in the range of 0–70% relative humidity at ambient (22 °C). In Figure 2 exemplary cyclic voltammetry results of the samples at 70% relative humidity and 5% relative humidity are shown for comparison. It is to be noted from an experimental point of view that we verified that the changes in memristance presented in Figure 2 are induced solely by the change of humidity and not by other atmospheric species, e.g., CO<sub>2</sub> or CO (see Figure S2, Supporting Information).

For a relative humidity >10% all three sets of samples show a pinched hysteretic behavior with counter-clockwise bipolar resistive switching typical for SrTiO<sub>3</sub>-based memristors<sup>[22a,24,48]</sup> as exemplarily shown for 70% relative humidity in Figure 2 (blue). This means the devices switches at positive polarity from high resistance state to low resistance state and by applying the opposite polarity the devices switch back to the high resistance state resetting the single Pt|SrTiO<sub>3</sub>|Pt bit. The hysteretic *I*–*V* profiles for all three sets of samples show an asymmetry as typical for such devices;<sup>[49]</sup> i.e., at positive bias the SET currents, *I*<sub>SET</sub>, are up to five orders of magnitude higher than the reset currents, *I*<sub>RESET</sub>, at negative bias. For constant experimental conditions the hysteretic behavior of a single bit was stable and showed no degradation over cycling, shown exemplarily by ten consecutive cycles for a given condition in Figure 2.

First we want to analyze the effect of the manipulated surface to bulk ratio on the exchange reaction with humid atmosphere by comparing the switching behavior of the *exposed HSBR* and *LSBR* samples (Figure 2 left and middle). Here, the asymmetry for positive and negative bias is more pronounced for the *HSBR* samples (Figure 2 middle) independent on the moisture exposure level when compared to the fourfold thicker *LSBR* devices (Figure 2 left). We explain this behavior by the enhanced influence of the Schottky barrier and the suppressed bulk

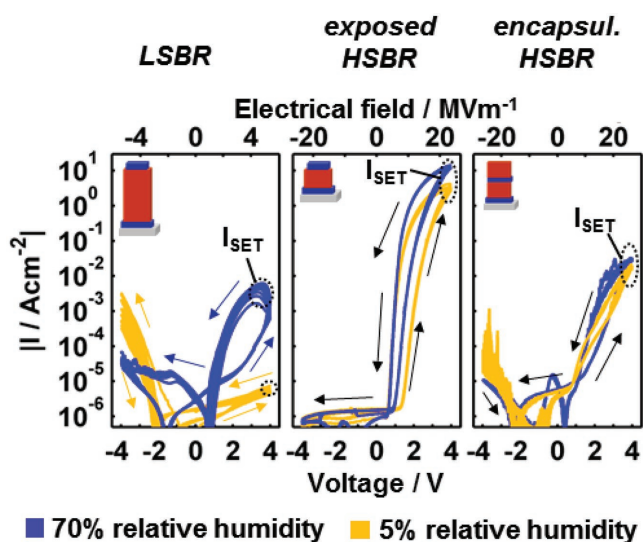


**Figure 2.** Exemplary cyclic voltammetry results of the three sets of samples measured in two extreme moisture exposure levels of 5% and 70% relative humidity. Each dataset shown here includes ten consecutive cycles indicating low variability in a constant atmosphere in contrast to the strong variation by moisture on the hysteretic behavior. LSBR: low surface to bulk ratio (740 nm film thickness); HSBR: high surface to bulk ratio (170 nm film thickness); encapsul.: encapsulated sample.

contribution of the HSBR SrTiO<sub>3</sub> devices. The HSBR devices showed in general a higher current density at positive voltage in the range of 1 A cm<sup>-2</sup> at +4 V and a lower high resistance to low resistance ratio, indicated by the smaller opening of the hysteresis, compared to the LSBR devices with a current density between 10<sup>-3</sup> to 10<sup>-6</sup> A cm<sup>-2</sup> at +4 V. The threshold SET voltage at which the current increases and the devices switch from their high to its low resistant state is for these cyclic voltammetry conditions for the HSBR samples at ≈1.3 V and for the LSBR samples at ≈2.4 V which corresponds to an electric field strength of 8 and 3 MV m<sup>-1</sup>, respectively. Both sets of samples showed expected<sup>[34a,43]</sup> higher  $I_{SET}$  conductivity at increased moisture exposure, but the HSBR set of samples is a lot less sensitive to moisture with a current density difference of one order of magnitude for a relative humidity change of 5–70% compared to the LSBR samples changing three orders of magnitude.

For low relative humidity in the range of 0–5% the LSBR sample this memristive behavior vanishes and only capacitive behavior is observed being in agreement to recent studies on SrTiO<sub>3</sub> and Ta<sub>2</sub>O<sub>5</sub>.<sup>[43,50]</sup> At these humidity levels the rectifying behavior is turned around and the sample gets more conductive at negative voltages as already observed in our earlier study.<sup>[43]</sup> This indicates that the inherent rectifying behavior of our LSBR samples is at least partially defined by the atmosphere and humidity exposure. Excitingly in addition to being less sensitive to moisture concerning  $I_{SET}$  the HSBR samples did still show hysteretic behavior and the memristance was preserved at these low moisture exposure levels in contrast to LSBR samples. These results show that bipolar resistive switching behavior occurs in SrTiO<sub>3</sub> over a wide range of 5–70% of relative humidity for oxide films and confirm that tuning of the surface to bulk ratio of the oxide leads to drastic changes in memristive response. These differences between the HSBR

and LSBR samples concerning their reaction to water exposure shown in Figure 2 can be either explained by a dominant role of the bulk in the memristive behavior which suits as an oxygen vacancy reservoir increasing the interaction toward moisture as the incorporation of protonic defects to the lattice is linked to the presence of the vacancies known from previous studies on the proton incorporation mechanism in SrTiO<sub>3</sub>.<sup>[15,37]</sup> Additionally the generally higher conductivity of the HSBR samples (≈1 A cm<sup>-2</sup>) could overlay the effects of moisture compared to the LSBR samples ( $\Delta_{5-70\%} \approx 10^{-3}$  A cm<sup>-2</sup>). These findings indicate that metal oxide thin films with a thickness closer to the Debye length are more suitable to suppress the moisture sensitivity for memory applications with the downside of smaller switching resistance off/on ratio (as known as the high resistance to low resistance states). But to exploit the moisture sensing behavior with a high sensitivity we report that Pt|SrTiO<sub>3</sub>|Pt memristive structures with a thicker active oxide layer around 750 nm seem to be beneficial for sensing applications.

Now we turn to the influence of moisture on memristance of *exposed* and *encapsulated* top electrodes to the atmosphere. Therefore we compare the  $I$ - $V$  profiles of HSBR sets of samples with equivalent thicknesses and microstructure but we define the atmospheric exposure level of the Pt|SrTiO<sub>3</sub>|Pt bits as either directly interacting with the atmosphere, *exposed HSBR* samples (Figure 2 middle), and one where the single bits are covered by an additional SrTiO<sub>3</sub> capping layer, *encapsulated HSBR* samples (Figure 2 right). Here, the  $I$ - $V$  profiles look qualitatively similar and all samples show stable memristive behavior in the relative humidity range of 5–70%. The *encapsulated HSBR* devices show similar to the *exposed LSBR* samples a lower current density of ≈10<sup>-2</sup> A cm<sup>-2</sup> at +4 V in comparison to the *exposed HSBR* devices with similar thickness with a current density around 10 A cm<sup>-2</sup> at +4 V. Therefore, we can conclude that the increased current density observed in this study for *exposed HSBR* samples cannot solely be attributed to reduced thickness but also to the atmosphere exposure. It has to be mentioned that the samples with the capping layer were fabricated via standard photolithography process and therefore chemisorbed water and protonic defects within the buried oxide layer are to be expected.<sup>[39,40]</sup> This explains why also all encapsulated LSBR memristor bits showed hysteretic  $I$ - $V$  profiles in contrast to the HSBR samples measured in dry atmospheres.

In contrast to the *exposed HSBR* samples, the *encapsulated HSBR* samples show no change of memristive behavior upon change to the relative humidity conditions in the range of 5–70% (see Figure 2 right). Also after long equilibration times of several days in humid atmosphere did the memristive behavior not change of the *encapsulated HSBR* Pt|SrTiO<sub>3</sub>|Pt devices during cyclic voltammetry experiments. This finding clearly shows: First, that the incorporation of protonic defects into the metal oxide layer is facilitated by the external applied electric field. Second, that the diffusion of protonic defects from the surface through the SrTiO<sub>3</sub> oxide thin film is limited and sluggish if no external electrical field is applied to the memristive device at ambient. Third, it shows that by fabricating devices with a capping layer parasitic atmospheric influences can be controlled and avoided for final applications as pure memristive devices. However, chemical reactions of moisture dissociating to protons that get incorporated to the SrTiO<sub>3</sub> lattice interacting

with oxygen vacancies have clearly to be considered for capless memristor operations.

### 2.3. Assessment of Required Protonic Defect Concentration for Memristive Operation

Until now recent memristor studies on valence change oxide-based memories could show that in dry atmospheres memristors can lose their switching capabilities and that protonic defects have an important impact on memristive behavior as presented in Figure 2 (left). Nevertheless it remained unclear when the transition between memristive and pure capacitive behavior takes place. In this work we were able to directly observe this transition at a specific relative humidity level of 5% (see Figure 3). In this particular cyclic voltammetry measurement on *exposed LSBR* sample the relative humidity was set to 5% and the capacitive behavior was measured in the initial cycle, shown in Figure 2 (left). During cycling the humidity increased slightly in the chamber below the detection limit of the humidity sensor and the evolution of a slight hysteresis could already be observed. This signifies that already a small amount of water is enough to trigger the memristive behavior for this set of samples and the bipolar hysteretic behavior is restored. In addition, it demonstrates that our structures under switching conditions show importantly a sensitivity limit toward moisture which is below standard ceramic based humidity sensors, <10% relative humidity.<sup>[32]</sup>

### 2.4. Reset Behavior as Function of Relative Humidity

It is important to note that not only the set processes at positive bias are affected by moisture induced effects but also the reset process at negative bias is influenced by changes in the relative humidity. Even though the  $I_{\text{RESET}}$  dependency upon moisture at  $-4$  V was weaker and more variable as the  $I_{\text{SET}}$  during the change of humidity in general an increased  $I_{\text{RESET}}$  could be measured in this study at higher relative humidity. But more interestingly the typical nonmonotonous conductivity decrease

during the resetting is strongly reduced at drier atmospheres (see Figure 4). Valov and co-workers<sup>[50]</sup> attributed this feature in cyclic voltammetry experiments on the example of  $\text{TaO}_x$  as switching oxide to the partial reoxidation, passivation, of the filaments resulting in a first resistance increase in the device. Our results indicate that this behavior is also strongly interfering with the protonic defects present and is not restricted to the discussion of oxygen vacancy filaments only. We hypothesize that it could even be that not the reoxidation of filaments but the rearrangement of protonic defects is the source of this relaxation process in the device.

### 2.5. Memristive Moisture Sensitivity for Sensing Application

Now we want to analyze this newly found sensitivity to moisture in dependence of the surface to bulk ratio of the oxide film during cycling voltammetry experiments in more detail. Therefore we systematically varied the relative humidity stepwise over a broad range of 0–80%. Figure 5 shows clearly the drastic change of the SET current density,  $I_{\text{SET}}$ , at +4 V upon moisture level exposure in dependence of the surface to bulk ratio showing the following characteristics for *exposed LSBR*, *exposed HSBR*, and *encapsulated HSBR* samples: Here, the *exposed LSBR* samples were very sensitive toward moisture and showed an exponential dependency of  $I_{\text{SET}}$  (Figure 5a), whereas the *exposed HSBR* samples only show a linear increase of  $I_{\text{SET}}$  by increasing the relative humidity (Figure 5a,b). This conductivity sensitivity toward moisture of Pt|SrTiO<sub>3</sub>|Pt bits presented here were fully reversible and could be measured over several humidity cycles (see Figure S3, Supporting Information). Here, a faster response time was measured for the *exposed LSBR* samples, which means the conductivity was increasing faster by increasing the relative humidity compared to recovery time when the relative humidity was decreased again. Importantly, we clearly demonstrate that the *encapsulated HSBR* samples showed no change in conductivity with respect to humidity for the range of 5–60% (see Figure 5b). It is noteworthy that for all samples the specific conductivity values given in Figure 5 measured at a constant relative humidity are strongly dependent

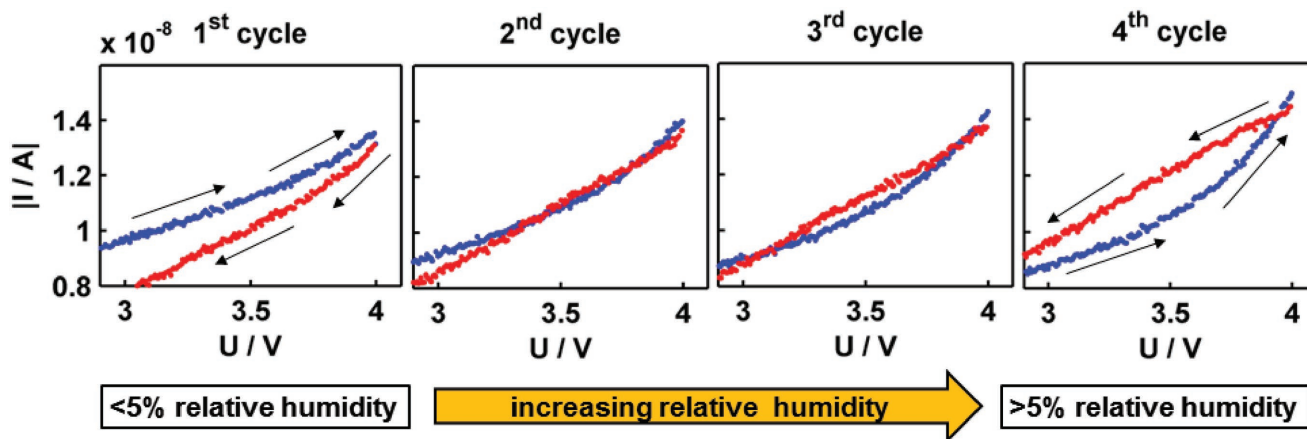


**Figure 3.** A closer look at cyclic voltammetry measurements for low moisture level ( $\approx 5\%$  relative humidity) shows that the transition of capacitive like behavior at low moisture levels toward hysteretic resistive switching behavior occurs already at 5% relative humidity for the exposed LSBR samples (film thickness = 740 nm).

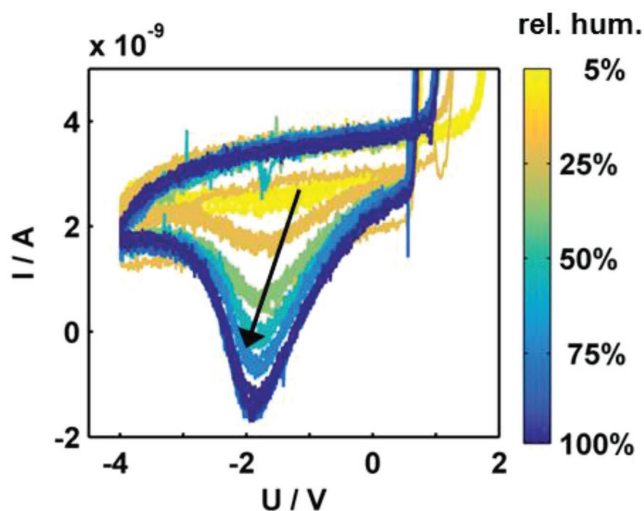


**Figure 4.** Analysis of the reset process in cyclic voltammetry experiments of the exposed HSBR SrTiO<sub>3</sub> sample shows an enhanced reaction for higher relative humidity in this voltage region.

on the measurement conditions during the cyclic voltammetry experiments like the sweep rate, in this work always kept at 50 mV s<sup>-1</sup>, which is an intrinsic property of memristors.<sup>[17,22a]</sup> These results show that by tuning the oxide film thickness the

sensitivity can be suppressed by using oxide layer thickness close to the Debye length,  $\approx 100$  nm, but also be enhanced by an oxide layer thickness far away of it. In addition, the specific conductivity values of such memristive humidity sensitive devices can be tuned by the sweep rate applied. This drastic enhancement and reversible change in the  $I_{SET}$  behavior could be potentially exploited for future ceramic humidity sensors but as presented in this work also in totally new device hybrids where memory can be stored and the humidity be sensed even within a single Pt|SrTiO<sub>3</sub>|Pt memristive bit.

In this study, they presented strong dependency of the conductivity of memristors on the moisture level during the SET and RESET process has severe implications on further research on such devices, e.g., the understanding of the underlying fundamental memristive mechanism as well on new device designs and potential synergistic memristive/sensor applications. We summarize in **Figure 6** a model on the interplay of moisture exposure with metal-oxide thin films under high electric fields and its electric behavior:

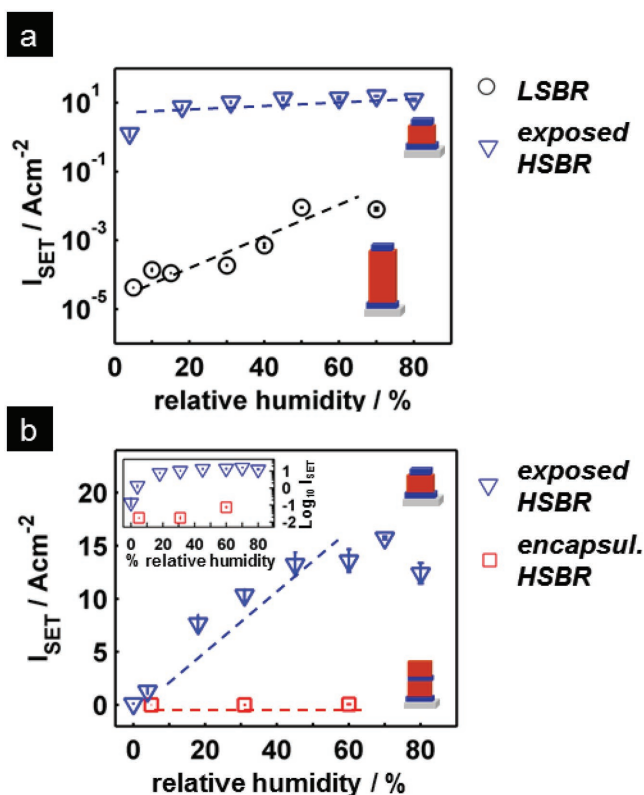


**Figure 5.** a) Current at SET voltage of +4 V,  $I_{SET}$ , for different moisture levels of LSBR sample shows an exponential behavior in contrast to a linear dependency of the exposed HSBR samples. b)  $I_{SET}$  of the encapsulated HSBR sample as reference specimen shows no change with moisture level.

- i) SrTiO<sub>3</sub> thin films directly exposed to the humid atmosphere with a thickness,  $d$ , larger than the Debye length,  $d \gg \lambda_d$ , react intensively and reversibly upon moisture exposure by modulation of the overall conductivity. Here two origins have to be considered. On the one hand side oxygen vacancies from the bulk, which acts as a defect reservoir, contribute to increased water dissociation at the Pt|SrTiO<sub>3</sub> interface in dependence of the atmospheric water concentration changing the adsorbed hydroxyl concentration at the interface. Even though the overall charge carrier concentration of the thin film stays constant upon water exposure, such surface charge changes are changing the Schottky barrier altering the overall electric behavior of the device (see Figure 6ai). In addition not only the surface charges could be intensively changed due to the oxygen vacancy reservoir but also increase the protonic defect incorporation and change the overall charged carrier concentration within the thin film as depicted in Figure 6aii.
- ii) SrTiO<sub>3</sub> thin films directly exposed to the humid atmosphere with a thickness,  $d$ , close to the Debye length,  $d \approx \lambda_d$ , react less intensively upon moisture exposure by modulation of the overall conductivity. As the thickness is decreased in such thin films and therefore the effect of the bulk is suppressed the sensitivity upon moisture is strongly decreased. Here, the water solely alters the electronic structure at the interface without changing the overall charge carrier concentration and modulates the Schottky barrier therein upon moisture exposure less without an accessible oxygen vacancy reservoir (see Figure 6b). Importantly, this increased incorporation of protonic defects does not take place without an external electric field. Here the total concentration of protonic defects remains unchanged independently of the moisture exposure.
- iii) SrTiO<sub>3</sub> thin films directly exposed to the humid atmosphere with a thickness,  $d$ , close to the Debye length,  $d \approx \lambda_d$ , does not react upon moisture exposure by modulation of the overall conductivity (see Figure 6c). Such a capping layer could be essential, as for the comparison and control of oxide-based valence change memristors it is essential to control the atmosphere during experiments and the protonic defects within the metal-oxide thin film.

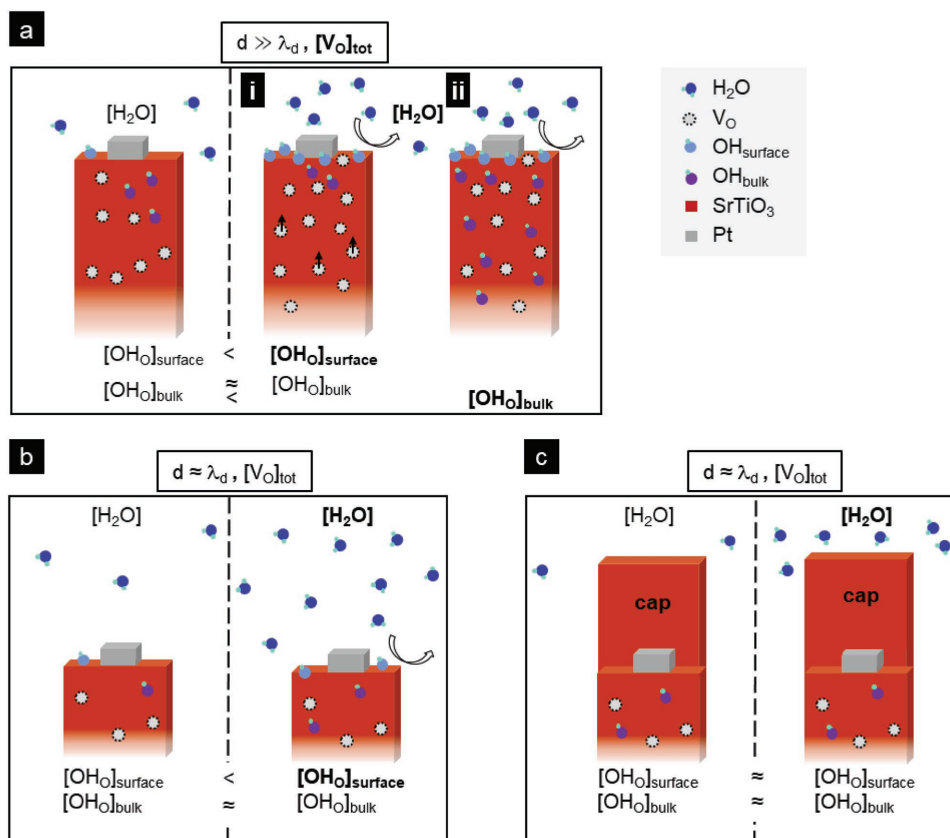


**Figure 6.** Schematic overview of the interplay of moisture exposure and the metal-oxide thin film under high electric fields and its electric behavior. a) SrTiO<sub>3</sub> thin films with a thickness larger than the Debye length,  $d \gg \lambda_d$ , react reversible with moisture exposure. Here, oxygen vacancies from the bulk, which acts as a defect reservoir, contribute either to an increased water incorporation at the Pt|SrTiO<sub>3</sub> interface as hydroxyl species changing the Schottky barrier altering the electric behavior (i). Potentially these oxygen vacancies from the bulk could also be responsible for an overall increased incorporation of protonic defects within the thin film (ii). b) For an oxide film thickness close to the Debye length,  $d \approx \lambda_d$ , the water alters the electronic structure at the interface solely and changes the Schottky barrier therein upon moisture exposure. c) An oxide capping layer prevents such an increased incorporation of protonic defects without an external electric field applied resulting in a moisture insensitive memristive behavior.

Additionally the presented results show that the resistive switching cannot be purely explained by the interaction of oxygen vacancies with the external electrical field but additionally the interplay with protonic defects has to be taken into consideration in all resistive switching models as these oxides are highly moisture sensitive. As shown in this study by the memristive oxide thickness dependency close and far from the Debye length the sensitivity toward humidity can be controlled. Importantly, the overall oxygen vacancy concentration in the bulk is defining the protonic contribution during memristive operation. This highly sensitive moisture dependency can be even leveraged for novel device applications where memristance and moisture sensing is possible within one single device structure as suggested memristive humidity sensors.

### 3. Conclusion

In this work, we create model devices to probe the implication of protonic defects on the property of memristance for which we actively modulate the surface to bulk ratio and the oxide surface exposure on the exchange with humid atmosphere.

Therefore, we study on either freely exposed or encapsulated Pt|SrTiO<sub>3</sub>|Pt model devices the memristance upon different relative humidity levels and vary in a systematic manner the memristive oxide thickness close and far from Debye length ( $\lambda_{d,SrTiO_3} \approx 100$  nm). By this approach we could assure that the total number of defects within the oxide is significantly different as well as the surface to bulk ratio and the oxide surface exposure toward the atmosphere without changing the underlying memristive mechanism.

We newly demonstrate based on this model experiment that one can couple humidity sensing to the property of memristance for the boundary condition that the oxide film thickness is far from the Debye length of the oxide material on the one hand and also that the incorporation and the release of protons is dominated by the oxygen vacancy reservoir being reversibly accessible from the oxide thin film. This is an interesting perspective for which we highlight on the one hand that if there is a free surface for the electrode the local electric field strength can be used to promote the water dissociation reaction. Excitingly, the model experiment by changing the memristive oxide film thickness reveals that there is a threshold upon which the sensitivity of

the memristive-sensor can be tuned from a linear to exponential dependency here demonstrated for an oxide thickness of 170 and 740 nm, respectively.

For classic memristor applications fundamentals of this study unequivocally demonstrate that protonic defects stemming from ambient and various levels of humidity need to be accounted for memristor characteristics as they crucially influence the switching characteristics and as shown in the low humidity experiments a necessary species for memristors. Nevertheless, simple capping as shown in a proof-of-concept clearly leads to stable performance.

In conclusion, model Pt|SrTiO<sub>3</sub>|Pt structures demonstrate clearly for the first time the *opportunity to create humidity sensors using the property of memristance* as a functional variable and characteristic. This opens a whole plethora of new modulatable sensor characteristics which extend classic resistive based oxide humidity tracking on the following aspects like controllable sensitivity from linear to exponential dependency, specific current values addressable in dependency of the sweep rate for a given humidity level and storing information within a single simple device structure.

## 4. Experimental Section

**Memristor Fabrication and Structural Characterization:** The memristors were fabricated on randomly cut sapphire substrates (Stettler, Switzerland) with a diameter of  $\varnothing = 35$  mm. The electrodes were fabricated through standard photolithography process in an International Organization for Standardization (ISO) 4 class cleanroom. Here, AZ nLOF 2070 (1:0.4) negative photoresist (Microchemicals, Germany) was dripped onto the substrate and spun with 4750 rpm for 45 s. The photoresist was then soft baked at 110 °C for 180 s with a rehydration step in air of at least 10 min. Afterward the electrode pattern was put on by illuminating the photoresist with UV light (constant energy mode of 210 mJ cm<sup>-2</sup>) with a mask aligner (Karl-Zeiss MJ3B) through customized designed foil masks (Selba, Switzerland). A post bake by 110 °C for 180 s was applied. In the end the photoresist was developed with MIF 726 developer for 90 s and rinsed in H<sub>2</sub>O. Prior to electrode deposition the patterned substrate was cleaned for 60 s at 100 W in an O<sub>2</sub> plasma asher (Technics Plasma TePla 100 Asher system). The 80 nm thick platinum bottom electrodes with a 5 nm titanium adhesion layer were deposited via electron beam evaporation (Plassys MEB 550). The final lift off was done in acetone. The top electrodes were fabricated alike without deposition of the titanium adhesion layer. The electrodes consisting of the crosspoints of bottom and top electrode have an area of 500 μm × 500 μm for the samples without a capping layer and 50 μm × 50 μm for samples with a SrTiO<sub>3</sub> capping layer. The relatively large electrode sizes (500–50 μm) allow to measure resistive switches with low statistical variations between devices in switching performance due to a homogenous defect distribution.

For the preparation of the strontium titanate, SrTiO<sub>3</sub>, target for the pulsed laser deposition (PLD) commercial SrTiO<sub>3</sub> (>99.5%, Aldrich Chemistry) was uniaxial pressed in a  $\varnothing = 3$  cm steel press mold with 140 kN for 150 s. Additionally the green body was isostatically pressed in an oil press for 2 min with 1000 kN. The target was thereon sintered for 5 h at 1350 °C with a heating/cooling rate of 2 K min<sup>-1</sup>. The SrTiO<sub>3</sub> thin film layers were deposited via pulsed laser deposition (Surface Advanced PLD technology; KrF excimer laser, 248 nm) at 650 °C with a heating rate of 10 K min<sup>-1</sup> at a pressure of 0.0267 mbar under a constant oxygen flow. The energy laser density was 0.6 J cm<sup>-2</sup> with a deposition frequency of 10 Hz. The thickness of the thin films was measured by profilometer measurements (Dektak XT Advanced profilometer, Bruker) directly after

deposition. Additionally was the thickness and microstructure confirmed by taking scanning electron microscopy (LEO 1530, Zeiss) images of cross-sections after electrical characterization with an acceleration voltage of 3 kV. For this, the samples were cleaved by a diamond pen and a 5 nm platinum layer was sputtered on the prepared samples to avoid charging. Additionally were all thin film samples characterized by X-ray diffraction (Bruker, D8, Cu K<sub>α</sub>) confirming the cubic perovskite crystal structure of pure SrTiO<sub>3</sub>.

**Probing Memristance under Different Relative Humidity Levels:** All electrical measurements were carried out using impedance bridges being a Solatron 1260 and 1287 (Ametek Ultra Precision Technologies), as well as a Gamry Reference 600 (Gamry Instruments). To prevent any permanent damage to the samples a compliance current of 5 mA was set. If not otherwise stated in the paper the cyclic voltammetry was done in the voltage range of ±4 V with a constant sweep rate of 50 mV s<sup>-1</sup>. The microelectrodes were contacted via custom-made platinum contact needles with a diameter of ≈20 μm which were positioned by manually controlled micro positioners employing a stereo light microscope (Nikon SMZ 1500). The top electrodes were set as the working electrode and the bottom electrode was set to ground. Every set of electrodes measured was initially stabilized before any further measurements by cycling it 25 times between ±4 V under laboratory conditions where typically a slight decrease in conductivity over cycling was observed before a stable behavior was achieved. This is in agreement with our observations reported earlier, see reference.<sup>[22a]</sup> The measurements were conducted in a closed custom made high vacuum microprobe stations (Everbeing Taiwan and Electrochemical Materials ETH Zurich Switzerland). The temperature during all measurements was kept constant at 22 ± 2 °C. The relative humidity inside the vacuum chamber was increased by guiding dry synthetic air (20% O<sub>2</sub>, 80% N<sub>2</sub>, H<sub>2</sub>O < 3 ppm) through a gas wash bottle containing H<sub>2</sub>O before being guided in the chamber. To decrease the relative humidity the synthetic air was directly guided into the chamber, after changing the moisture level inside the chamber the samples were equilibrated at least for 30 min prior measurements. The relative humidity was measured with an accuracy of ±2% by a humidity sensor (SHT21, Sensirion) placed inside of the chamber. It was verified that the changes are induced by the change of humidity and not by other changes in the atmosphere by setting the humidity level to the same value in the synthetic air as present in the laboratory (see Figure S2, Supporting Information). Here, during cyclic voltammetry experiments the exact same behavior was measured for both atmospheres. Therefore effects from other minor gases present in laboratory air can be ruled out and the further discussion can be solely restricted to changes in humidity.

## Supporting Information

Supporting Information is available from the Wiley Online Library or from the author.

## Acknowledgements

The authors thank Eva Sediva for preparing the microelectrodes for the encapsulated samples. This work was supported by Swiss National Science Foundation Projects, Grant Nos. 138914, 155986, and 144988. F.M. and M.J. prepared the samples. M.J. performed the electrical characterization. F.M. performed the analysis of the electrical results. F.M. and J.L.M.R. cowrote and edited the paper. All authors contributed to discussions about the paper.

## Conflict of Interest

The authors declare no conflict of interest.

## Keywords

humidity, memristors, oxygen ionic conductivity, protonic conductivity, resistive switching, resistive random access memory, strontium titanate

Received: May 4, 2018

Revised: July 30, 2018

Published online: September 17, 2018

- [1] International Technology Roadmap for Semiconducting Industry (ITRS), <http://www.itrs2.net/itrs-reports.html> (accessed: October 2015).
- [2] D. B. Strukov, G. S. Snider, D. R. Stewart, R. S. Williams, *Nature* **2008**, 453, 80.
- [3] L. O. Chua, *IEEE Trans. Circuits Syst.* **1971**, Ct18, 507.
- [4] L. O. Chua, S. M. Kang, *Proc. IEEE* **1976**, 64, 209.
- [5] S. Vongehr, X. Meng, *Sci. Rep.* **2015**, 5, 11657.
- [6] The term memristor and memristance is used in this work as it is customary in the resistive switching community, even though the authors are aware of that there is an ongoing discussion if these devices are real memristors, memristive devices or nothing of all.
- [7] a) Z. Wang, M. Yin, T. Zhang, Y. Cai, Y. Wang, Y. Yang, R. Huang, *Nanoscale* **2016**, 8, 14015; b) S. H. Jo, T. Chang, I. Ebong, B. B. Bhadviya, P. Mazumder, W. Lu, *Nano Lett.* **2010**, 10, 1297; c) Z.-H. Tan, R. Yang, K. Terabe, X.-B. Yin, X.-D. Zhang, X. Guo, *Adv. Mater.* **2016**, 28, 377; d) C. Wu, T. W. Kim, H. Y. Choi, D. B. Strukov, J. J. Yang, *Nat. Commun.* **2017**, 8, 752.
- [8] R. Waser, R. Dittmann, G. Staikov, K. Szot, *Adv. Mater.* **2009**, 21, 2632.
- [9] Y. V. Pershin, M. Di Ventra, *Adv. Phys.* **2011**, 60, 145.
- [10] N. Raghavan, *Microelectron. Reliab.* **2014**, 54, 2253.
- [11] Y. Yang, X. Zhang, L. Qin, Q. Zeng, X. Qiu, R. Huang, *Nat. Commun.* **2017**, 8, 15173.
- [12] a) J. Crawford, P. Jacobs, *J. Solid State Chem.* **1999**, 144, 423; b) A. Walsh, C. R. A. Catlow, A. G. H. Smith, A. A. Sokol, S. M. Woodley, *Phys. Rev. B* **2011**, 83, 220301.
- [13] a) R. A. Cowley, *Philos. Trans. R. Soc., A* **1996**, 354, 2799; b) R. Perez-Casero, J. Perrière, A. Gutierrez-Llorente, D. Defourneau, E. Millon, W. Seiler, L. Soriano, *Phys. Rev. B* **2007**, 75, 165317.
- [14] R. A. De Souza, J. Fleig, R. Merkle, J. Maier, *Z. Metallkd.* **2003**, 94, 218.
- [15] R. Merkle, J. Maier, *Angew. Chem., Int. Ed.* **2008**, 47, 3874.
- [16] S. Lee, J. S. Lee, J. B. Park, Y. K. Kyoung, M. J. Lee, T. W. Noh, *APL Mater.* **2014**, 2, 066103.
- [17] S. Menzel, M. Waters, A. Marchewka, U. Bottger, R. Dittmann, R. Waser, *Adv. Funct. Mater.* **2011**, 21, 4487.
- [18] D. J. Seong, M. Jo, D. Lee, H. Hwang, *Electrochem. Solid-State Lett.* **2007**, 10, H168.
- [19] S. Y. Dai, H. B. Lu, F. Chen, Z. H. Chen, Z. Y. Ren, D. H. L. Ng, *Appl. Phys. Lett.* **2002**, 80, 3545.
- [20] M. Wojtyniak, K. Szot, R. Wrzalik, C. Rodenbacher, G. Roth, R. Waser, *J. Appl. Phys.* **2013**, 113, 083713.
- [21] a) R. Muenstermann, T. Menke, R. Dittmann, R. Waser, *Adv. Mater.* **2010**, 22, 4819; b) T. Menke, R. Dittmann, P. Meuffels, K. Szot, R. Waser, *J. Appl. Phys.* **2009**, 106, 114507.
- [22] a) F. Messerschmitt, M. Kubicek, S. Schweiger, J. L. M. Rupp, *Adv. Funct. Mater.* **2014**, 24, 7448; b) H. Nili, S. Walia, A. E. Kandjani, R. Ramanathan, P. Gutruf, T. Ahmed, S. Balendhran, V. Bansal, D. B. Strukov, O. Kavehei, M. Bhaskaran, S. Sriram, *Adv. Funct. Mater.* **2015**, 25, 3172.
- [23] a) M. C. Ni, S. M. Guo, H. F. Tian, Y. G. Zhao, J. Q. Li, *Appl. Phys. Lett.* **2007**, 91, 183502; b) W. Jiang, M. Noman, Y. M. Lu, J. A. Bain, P. A. Salvador, M. Skowronski, *J. Appl. Phys.* **2011**, 110, 034509.
- [24] M. Kubicek, R. Schmitt, F. Messerschmitt, J. L. M. Rupp, *ACS Nano* **2015**, 9, 10737.
- [25] K. Shibuya, R. Dittmann, S. B. Mi, R. Waser, *Adv. Mater.* **2010**, 22, 411.
- [26] Z. A. Ansari, T. G. Ko, J. H. Oh, *Surf. Coat. Technol.* **2004**, 179, 182.
- [27] a) M. Shirpour, G. Gregori, R. Merkle, J. Maier, *Phys. Chem. Chem. Phys.* **2011**, 13, 937; b) E. Ruiz-Trejo, J. A. Kilner, *J. Appl. Electrochem.* **2009**, 39, 523; c) S. Kim, H. J. Avila-Paredes, S. Wang, C. T. Chen, R. A. De Souza, M. Martin, Z. A. Munir, *Phys. Chem. Chem. Phys.* **2009**, 11, 3035.
- [28] Y. C. Yeh, T. Y. Tseng, D. A. Chang, *J. Am. Ceram. Soc.* **1989**, 72, 1472.
- [29] Y. He, T. Zhang, W. Zheng, R. Wang, X. W. Liu, Y. Xia, J. W. Zhao, *Sens. Actuators, B* **2010**, 146, 98.
- [30] S. G. Ansari, Z. A. Ansari, M. R. Kadam, R. N. Karekar, R. C. Aiyer, *Sens. Actuators, B* **1994**, 21, 159.
- [31] a) T. Seiyama, N. Yamazoe, H. Arai, *Sens. Actuators* **1983**, 4, 85; b) Z. Chen, C. Lu, *Sens. Lett.* **2005**, 3, 274; c) E. Traversa, *Sens. Actuators, B* **1995**, 23, 135.
- [32] T. A. Blank, L. P. Eksperianova, K. N. Belikov, *Sens. Actuators, B* **2016**, 228, 416.
- [33] a) D. Poetzsch, R. Merkle, J. Maier, *Adv. Funct. Mater.* **2015**, 25, 1542; b) K. D. Kreuer, *Annu. Rev. Mater. Res.* **2003**, 33, 333.
- [34] a) W. Qu, R. Green, M. Austin, *Meas. Sci. Technol.* **2000**, 11, 1111; b) Y. Yamazaki, P. Babilo, S. M. Haile, *Chem. Mater.* **2008**, 20, 6352; c) R. B. Cervera, Y. Oyama, S. Miyoshi, I. Oikawa, H. Takamura, S. Yamaguchi, *Solid State Ionics* **2014**, 264, 1; d) Q. Chen, F. El Gabaly, F. Aksoy Akgul, Z. Liu, B. S. Mun, S. Yamaguchi, A. Braun, *Chem. Mater.* **2013**, 25, 4690; e) E. Fabbri, L. Bi, D. Pergolesi, E. Traversa, *Adv. Mater.* **2012**, 24, 195.
- [35] E. C. C. d. Souza, R. Muccillo, *Mater. Res.* **2010**, 13, 385.
- [36] S. Agarwal, G. L. Sharma, R. Manchanda, *Solid State Commun.* **2001**, 119, 681.
- [37] a) S. Steinsvik, *Solid State Ionics* **2001**, 143, 103; b) R. Waser, *Ber. Bunsenges. Phys. Chem.* **1986**, 90, 1223.
- [38] J. H. Yu, J. S. Lee, J. Maier, *Angew. Chem., Int. Ed.* **2007**, 46, 8992.
- [39] D. Hrabovský, B. Berini, A. Fouchet, D. Aureau, N. Keller, A. Etcheberry, Y. Dumont, *Appl. Surf. Sci.* **2016**, 367, 307.
- [40] D. Shang, S. Lee, Y. Sun, *Solid State Ionics* **2016**, 295, 1.
- [41] a) J. R. Jameson, Y. Nishi, *Integr. Ferroelectr.* **2011**, 124, 112; b) Q. Yin, C. Wei, Q. Wei, Y. Chen, Y. Xia, B. Xu, J. Yin, Z. Liu, *Appl. Phys. Express* **2016**, 9, 104202.
- [42] Y. F. Chang, B. Fowler, Y. C. Chen, F. Zhou, C. H. Pan, T. C. Chang, J. C. Lee, *Sci. Rep.* **2016**, 6, 21268.
- [43] F. Messerschmitt, M. Kubicek, J. L. M. Rupp, *Adv. Funct. Mater.* **2015**, 25, 5117.
- [44] T. Tsuruoka, I. Valov, C. Mannequin, T. Hasegawa, R. Waser, M. Aono, *Jpn. J. Appl. Phys.* **2016**, 55, 06GJ09.
- [45] Y. Qiaonan, W. Chunyang, X. Yidong, X. Bo, Y. Jiang, L. Zhiguo, *J. Phys. D: Appl. Phys.* **2016**, 49, 09LT01.
- [46] a) Z. Mao, R. E. Dunin-Borkowski, C. B. Boothroyd, K. M. Knowles, *J. Am. Ceram. Soc.* **1998**, 81, 2917; b) R. Waser, *Ferroelectrics* **1994**, 151, 125.
- [47] R. A. De Souza, J. Fleig, J. Maier, O. Kienzle, Z. Zhang, W. Sigle, M. Rühle, *J. Am. Ceram. Soc.* **2003**, 86, 922.
- [48] J. Park, D.-H. Kwon, H. Park, C. U. Jung, M. Kim, *Appl. Phys. Lett.* **2014**, 105, 183103.
- [49] S. Menzel, R. Waser, *Phys. Status Solidi RRL* **2014**, 8, 540.
- [50] M. Lübben, P. Karakolis, V. Ioannou-Sougliridis, P. Normand, P. Dimitrakakis, I. Valov, *Adv. Mater.* **2015**, 27, 6202.